RSC Advances

ROYAL SOCIETY OF CHEMISTRY

www.rsc.org/advances

Journal Name

ARTICLE

The luminescence inner filter effect of Mn^{2+}-doping $(ZnS)_2$·octylamine inorganic/organic hybrid thin films and its sensor application for environmental contaminants

Received 00th January 20xx,
Accepted 00th January 20xx

DOI: 10.1039/x0xx00000x

www.rsc.org/

Yu Chen,[a] Jinhui Wang,[a] Jing Li,[a] Xinxin Li,[b] and Shuo Wei*[a]

II–VI group/monoamine hybrid was one of novel inorganic/organic (I/O) layered structures and exhibited strong quantum confinement effect and well-defined Mn^{2+}-doping luminescence, which was imperative and valuable academically for its application. In this work, the pure and well-crystalline $(ZnS:Mn)_2$·*oa* (*oa* = octylamine) hybrid was prepared by solvothermal synthesis and its thin films was fabricated by drop-casting method. The 5 at% Mn^{2+}-doping hybrid exhibited a strong Mn^{2+} luminescence at 597 nm with the 300 nm excitation. The inner filter effect(IFE) for this luminescence was investigated and verified by detecting three selected environmental contaminant species, n-butyl xanthate(BX), crystal violet (CV), and reaction black 5 (RB5), which indicated that this hybrid thin film has a good luminescence IFE-based linear response for the μM species solution. Furthermore, the 597 nm luminescence remain intact for the solution with pH = 4 to 10 and the hydrophobicity of the hybrid thin film was favorable for its rapid and multiple IFE-based detection. Therefore, this hybrid thin film is a competitive candidate for new-generational fluorescence sensor to probe occurrence of these environmental contaminants.

1.Introduction

Nowadays, the development of novel fluorescence-based assays sensor device has received intensive and continuing attention owing to the distinct advantages of inherent sensitivity, nondestruction, suitability for microscopic imaging, low-cost and structural diversity. There is an enormous demand for a luminescence-based sensing method in many fields such as environmental monitoring, industrial and food processing, biomedical technology, healthcare, and clinical analysis. The fluorescence inner filter effect (IFE) is a kind of fluorescence quench mechanism originated from the absorption of the excitation and/or emission light of the fluorescence species by the absorbent species, which was usually treated as an annoying source of error in spectrofluorometry.[1,2] Oppositely, this effect can be designed as a fluorescence senor method, in which an optical absorbent and a fluorophore are employed and the absorption band of the former, to some extent, overlap with the excitation and/or emission bands of the latter. That is, the analytic absorption signal is conversed to the fluorescence signal of the luminescence species within the fluorescence IFE. And the efficiency is related to the spectral overlap and optical absorption ability. Compared to the conventional fluorescence assays, including kinetic/static quench or nonradiative/resonance energy transfer (PET, EET, FRET) and charge transfer (TICT, ICT, MLCT), the IFE is simple and preferred, without the proximity at nanoscale between an absorbent and a fluorophore. Since the pioneered work of Cary in 1984,[3] IFE-based fluorescence sensors have witnessed a fast development to detect various chemical and biological analytes, ranging from meal ions/anions to protease, and single nucleotide polymorphisms.[4-8]

The inorganic/organic (I/O) hybrid compounds are a kind of composites with the inorganic and organic component combination at atomic level, which have the advantages in inorganic rigidity, stability and organic lightweight, flexibility, processability, diversity.[9,10] Furthermore, they possess unique electronic/optical properties being attributed to their individual constituents, and have become new-generational functional materials and research focus of materials sciences for more than 30 years.[11-14] Firstly reported in 2003, the II–VI group/amine hybrid compounds were novel type of I/O hybrid layered structures, with the chemical formula can be generalized as $(ME)_p(L)_q$(M = Zn, Cd, Mn; E = S, Se, or Te, *p*, *q* = 1 or 2, and L = aliphatic monoamines, diamines or hydrazine).[15] Due to their structural uniformity and periodicity, the II-VI group/amine hybrid compounds are particularly attractive. In these hybrids, the valence electrons are quantum confined to perform the modified semiconductor

[a] College of Chemistry, Beijing Normal University, 19 Xinjiekou Outside Street, 100875, Beijing ,China. E-mail: vshuo@bnu.edu.cn; Tel:+86-10-58802740
[b] Analytical and testing center, Beijing Normal University, 19 Xinjiekou Outside Street, 100875, Beijing ,China

† Electronic Supplementary Information (ESI) available: The cycle reversibility of the Mn^{2+} luminescence of the hybrid thin film responding to the BX(23.12μM) and RB5(8.739μM) aqueous solution, and the luminescence spectra of the hybrid thin film dipping into the blank aqueous solution with pH = 4 to 10. See DOI: 10.1039/x0xx00000x

properties into the inorganic II-VI group ME slabs, which was linked to the organic amine spacer layers by the M–N bonding. And both layers alternatively stacked in an ordered periodic way to form the layered structure.[15] Research of these hybrids show they include an intralayer structure,[14-18] thermal expansion behaviour,[19-21] pyrolysis properties,[22,23] DFT study of its energy band structure,[24,25] application in white-light light emission diode,[26-28] and photoelectric properties.[29-31] The room temperature UV optical absorption with typical band edge exciton feature exhibited a large blueshift compared with their II–VI semiconductor counterparts, which can be attributed to the strong quantum confinement effect (QCE)[15] of the ME inorganic slabs, and the hybrid can be regarded as a periodic multiple quantum well (MQW) structure. Furthermore, the Mn^{2+} substitutional doping provided the hybrid with a strong Stokes luminescence (2.12 eV, 586 nm) at room temperature.[16] It has been manifested that the luminescence intensity reached its maximum for the Mn^{2+} doping atomic percentage at 0.05. As for device application, the spin-coating method was reported to fabricate the inorganic/organic hybrid luminescence films.[29] The $(ZnS:Mn)_2$·monoamine I/O hybrid compounds have good Mn^{2+} fluorescence, which can be applied into novel analytic probe and fluorescence sensor. It is interesting and important to study the quench mechanism of Mn^{2+} luminescence by various species, which is not only vital for the optical properties of this kind of hybrids academically, but also fundamental for its sensor application.

In this paper, based on the luminescence IFE, three representative molecule species, n-butyl xanthate(BX), crystal violet(CV), and reactive black 5(RB5)(see Scheme 1) were selected to test the IFE for the $(Zn_{0.95}Mn_{0.05}S)_2$·oa hybrid thin film with strong and well-defined Mn^{2+} luminescence (λ_{ex} = 300 nm, λ_{em} = 597 nm), because BX, CV, and RB5, have matched optical absorption for the excitation, emission or both maximum of the film's fluorescence, respectively. BX is one of the important flotation reagents in metallurgy, and it reeks severely with a destructive impact to fishes.[32] The CV iss used as low-cost aquaculture fungicide in piscatory, which seriously affect the food safety,[33] and RB5 is one of the typical azo dyes in the industrial waste water.[34] They are all water-soluble anions and harmful to the water environment and ecosystem. At present the most common detection methods of these three molecules are the ultraviolet absorption spectrophotometric method, liquid chromatography and liquid chromatography-mass spectrometry. All of these are instrumental demanding and there is an enormous demand for an efficient and simple analytical method to detect these three molecules.

Firstly, $(Zn_{0.95}Mn_{0.05}S)_2$·oa hybrid was prepared by solvothermal synthesis. Its fluorescence properties was characterized, which indicated a strong excitation peak at 300 nm and the Mn^{2+} fluorescence at 597 nm, and the optimal fluorescence was obtained at the 5 at% Mn^{2+} doping content, which was employed as the luminescence probe for the three species. The linear relationship between the luminescence intensity and the concentration was established at μM level.

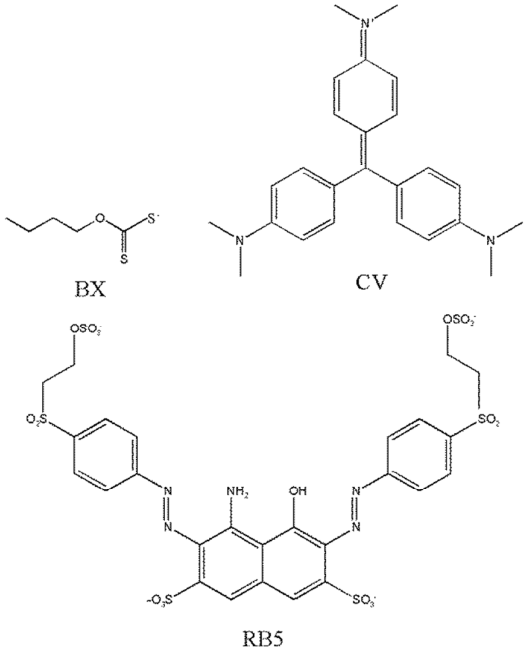

Scheme 1 Three environmental contaminants for investigating the luminsecence IFE of the hybrid thin film

2.Experimental

2.1 Reagents and Materials

Octylamine ($C_8H_{19}N$) was purchased from Aladdin Chemical. Co. Ltd. Analytical grade $Mn(Ac)_2·4H_2O$, $Zn(Ac)_2·2H_2O$, S, C_2H_5OH, $CH_3CO_2C_2H_5$ were purchased from Beijing Chemical Co. Ltd. Potassium butyl xanthate(BX, $C_5H_9OS_2K$, 188.3527), Crystal violet(CV, $C_{25}H_{30}N_3Cl·9H_2O$, 407.98), and reactive black 5(RB5, $C_{26}H_{21}N_5O_{19}S_6Na_4$, 991.8161), were purchased from J&K Chemical Co. Ltd. All these reagents were used without further purification. Deionized water was used in all the experimental processes.

2.2 Characterization

The X-ray diffraction patterns (XRD) of the films was recorded using a PANalytical X' Pert PRO MPD under the following conditions: 40 kV, 40 mA, and Cu Kα radiation (λ = 1.541844Å) with step scanning (0.0330°/2θ per step) in the range from 2 to 70° using a count time of 59.6900 s/step. The morphology and thickness of thin films were investigated by using a scanning electron microscope (SEM, Hitachi S-4800) and the accelerating voltage applied was 20 kV. The UV-vis absorption spectra were collected in the range from 260 to 700 nm on a Shimadzu UV-2450 spectrophotometer with the slit width of 1.0 nm. The steady state fluorescence excitation and emission spectra were performed on a PerkinElmer-LS55 fluorescence spectrophotometer, and both the excitation and emission slit are set to 6.0 nm, with the excitation at 300 nm. The fluorescence decay curves were recorded with the excitation at 300 nm from the Xe lamp.

2.3 Hybrid synthesis and thin film fabrication

2.3.1 Preparation of the hybrid compounds. $(Zn_{0.95}Mn_{0.05}S)_2$·oa were synthesized by the typical solvothermal method. Firstly, a solution of 35 mL octylamine(oa), 4.75 mmol $Zn(Ac)_2·2H_2O$, 0.25 mmol $Mn(Ac)_2·2H_2O$ and 5 mmol sulfur powder was mixed and magnetically stirred, then transferred into the 50 mL of Teflon-liner, which was lined into the autoclave, sealed and heated at 170°C for 5-7 days. After natural cooling to room temperature, the offwhite lamellar product was obtained by washed with deionized water and 90% absolute ethanol. Dry the product powder at 60°C in vacuum for the next step.

2.3.2 Fabrication of the hybrid thin film. The quartz substrate for thin film fabrication was cleaned by several procedures, firstly soaked in aqua regia, then ultrasonically rinsed sequentially with deionized water, H_2SO_4:30%H_2O_2 (3:1, v/v) mixture solution (40 min), and deionized water, respectively. Then the quartz plate was dipped and washed into the boiling ethanol for 10 min, and dried in vacuum oven for 3–10h. The hybrid suspension (2mg/mL) of the $(Zn_{0.95}Mn_{0.05}S)_2$·oa was obtained by ultrasonically dispersing in ethyl acetate for over 5 hours. Drop the as-prepared hybrid suspension on a neat treated quartz substrate with caution to ensure the suspension to coat the whole substrate homogenously, repeat this dropping for three times at least, then the thin film was standing still in the air until the solvent volatilized completely.

2.4 Fluorescence detection assays of CV, RB5 and BX

Micromolar concentration scale of CV, RB5 and BX aqueous solution were prepared by dissolving in deionized water, respectively. Then insert the hybrid thin films in a cross color dish with different concentration solutions. The fluorescence quenching of the thin film was recorded with the fluorescence spectroscopy.

3. Results and discussion

3.1 Structure and morphology characterization

XRD measurement was performed to check the periodic structure of as-prepared hybrid powder and thin film. The XRD patterns of the as-prepared hybrid and its drop-casting films were shown in Fig. 1A, in which a typical layered structure could be revealed with the first three Bragg diffraction peaks at 2.84° (001), 5.68°(002) and 8.49°(003), respectively, corresponding to a periodic space about 3.1 nm. This indicated that the hybrid powder and its thin film were pure and well crystalline. The 3.1 nm period implied the double-layered octylamine alignment between the inorganic $(ZnS)_2$ layers with the nonpolar octyl groups point opposite each other, like the cell menbrane, compared with the molecular length of *oa* (1.19 nm), which was similar to other hybrid homologs (such as, propylamine, butylamine and hexylamine).[7] Moreover, the film fabrication process held this layered crystalline structure intact. The subtle difference at 26 to 32°/2θ in the XRD between the powder and thin film (Fig. 1A inset) indicated that the thin film preferred orientation with the (001) crystalline

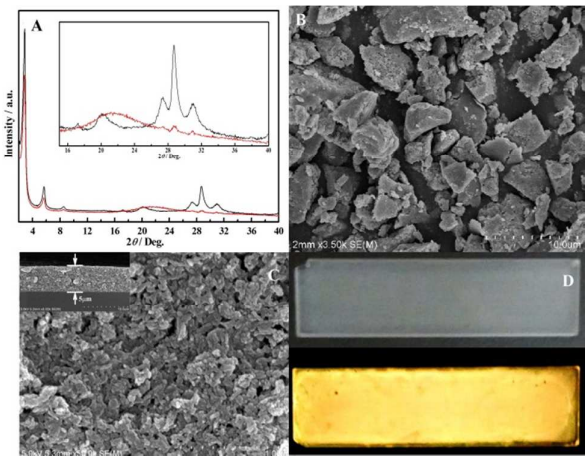

Figure1 . The structure and morphology characterization.(A) XRD of the hybrid powder (black profile) and the film (red profile), the inset was the enlarged section of 15-40° (2θ), (B) SEM images of the hybrid powder, (C) the photograph shows the surface of the thin film and the inset was the cross section of the film (D) the photograph of the thin film under daylight and UV light.

plane packing in the substrate, and other *hk*0 (*h,k* ≠ 0) Bragg peaks disappeared, which was typical for inorganic layered structure like graphite. The top-view SEM image (Fig. 1B) showed that the hybrid powders were irregular lump shape with micrometre size. The top-view SEM image of the as-prepared thin film (Fig. 1C) displayed the thin film was continuous, homogenous with small hybrid nanoparticles, and the inset showed the film thickness was 5 μm. These results confirmed the hybrid thin film fabricated by drop-casting method was structure-held and homogeneous and continuous. The as-prepared thin film on the quartz substrate exhibited strong orange luminescence under the UV illumination (Fig. 1D).

3.2 Optical properties of the hybrid film and selective determined species

Figure 2 showed that the hybrid film had a strong Mn^{2+} luminescence at 597 nm, with the maximum excitation at 300 nm. The three selective environmental contaminants BX, CV, and RB5 have the matched spectral overlap with the emission/excitation band of the hybrid thin film, to characterize the luminescence IFE. The absorption bond of BX ranged from 275 nm to 325 nm with the maximum peak at 300 nm (ε_{300} = 1.488×10^4 $M^{-1}·cm^{-1}$), which was selected to absorb the excitation light of the film. In the CV absorption spectroscopy, except the maximum absorbance in 582 nm (ε_{582} = 5.689×10^4 $M^{-1}·cm^{-1}$), which absorb the Mn^{2+} emission light, although there is also a relatively weak absorption at 300 nm (ε_{300} = 1.524×10^4 $M^{-1}·cm^{-1}$). As far as the RB5 is concerned, it has two broad peaks with similar intensity at 597 nm (ε_{597} = 4.122×10^4 $M^{-1}·cm^{-1}$) and 300 nm (ε_{300} = 2.576×10^4 $M^{-1}·cm^{-1}$), that is it absorbs both the emission and excitation light to the similar extent. Furthermore, it was found that the BX, CV, RB5 aqueous solution with μM concentration absorb the UV and visible light stably. Therefore, these three selected species represent the typical situations for investigating the luminescence IFE of the hybrid thin film.

3.3 The luminescence IFE of the selective species

The relationship between the Mn^{2+} luminescence intensity of the hybrid thin film and the aqueous concentration of three species was investigated for characterizing its IFE. Experimentally, this was realized by *in situ* detecting the luminescence intensity of the hybrid thin film when dipping into the species solution at certain concentration. Accordingly, the Mn^{2+} luminescence quench was observed in different extent, which could be attributed to the

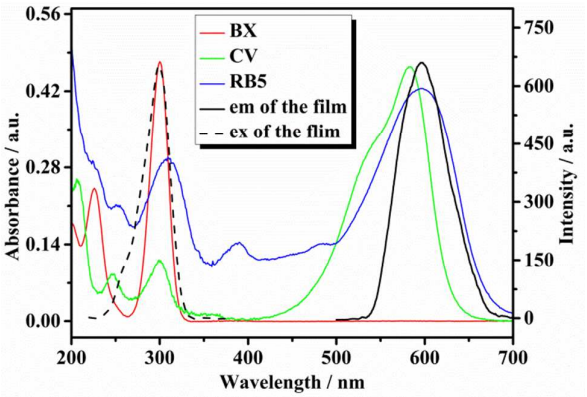

Figure 2. The photoluminescence excitation(dash black) and emission(solid black) spectra of the $(Zn_{0.95}Mn_{0.05})_2$·oa hybrid film. and the optical absorption spectra of the three selective environmental contaminants BX(red curve, 31.86μM), CV(green curve, 7.35μM) and RB5(blue curve, 10.08μM)

luminescence IFE of the three species to the $(Zn_{0.95}Mn_{0.05}S)_2$oa hybrid thin film. In order to reveal the prominent luminescence quench, the Mn^{2+} luminescence intensity at 582 nm was used to detect CV, while 597 nm was selected to detect the BX and RB5.

Figure 3 showed the logarithm of the luminescence intensity (Log *I*) vs. concentration(*c*) plots for the three selective species. The luminescence of the hybrid thin film fell gradually upon the concentration increasing of BX, CV and RB5 aqueous solution. A good linear relationship of the logarithm of fluorescence intensity to concentration was found (R^2, 0.981 to 0.994, see Table 1). All the linear fitting parameters for the three species were listed in Table 1. As shown in Table 1, the linear relationship held for different range of three species, with that of BX broadest (0 – 53.10 μM), RB5 in the middle (0 – 16.13 μM), and CV (0 – 11.03 μM) least. This trend is consistent with the extinction coefficients in the order of BX (ε_{300} = 1.488 × 10^4 M^{-1}·cm^{-1}), RB5 (ε_{597} = 4.122 × 10^4 M^{-1}·cm^{-1}, ε_{300} = 2.576 × 10^4 M^{-1}·cm^{-1}), and CV(ε_{582} = 5.689 × 10^4 M^{-1}·cm^{-1}). That is, the luminescence quench is more efficient for the absorption of the emission light than that of the excitation light. The absorption for both resulted in a narrow linear range for RB5. Beyond the upper ranges, the luminescence intensity deviated from the linear relation and could not be employed as the concentration detection of three species. On the other hand, the absolute value of the slope (|a|) of the fitting straight lines also exhibit the same trends as that of the linear range (CV > RB5> BX), which implied that this hybrid thin film has a best resolution for probing CV based on the luminescence IFE.

3.4 The Stern-Volmer plots of the Mn^{2+} luminescence of hybrid thin film

Luminescence quench is a typical character of the IFE. To further study the luminescence IFE of the hybrid thin film for the three species, the Stern-Volmer plots in their linear response ranges were illustrated. In Figure 4, the (I_0/I − 1) was plotted against the concentration(*c*) to be fitted as a straight line and all the fitting parameters were lilsted in Table 2. It could be found that for all the three speicies, the linear fitting could be obtained in the identical linear response range of Log*I*-*c* plot. The K_{SV} values is calculated to be 52320, 244100, 159200 L/mol for BX, CV and RB5, respectively,

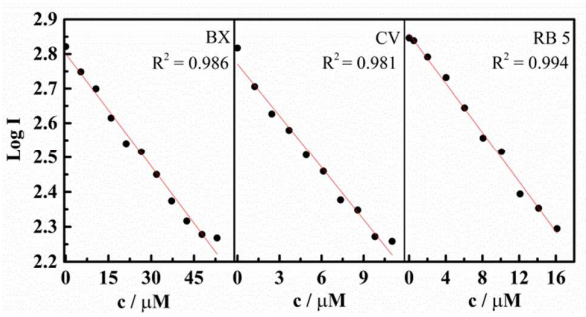

Figure 3. The Log *I* vs. concentration (c / μM, pH = 7) plot for the hybrid thin film

Table 1 The linear fitting parameter of the Log*I* vs. *c* plot in Figure 3

	a /($\times10^{-2}$)*	*b**	Linear range / μM	Molecular weight	R^2
BX	− 1.090	2.801	0 – 53.10	188.35	0.986
CV	− 4.998	2.771	0 – 11.03	407.98	0.981
RB5	− 3.570	2.858	0 – 16.13	991.82	0.994

* The fitting equation was Log *I* = *ac* + *b*, R^2, correlation coefficient

which indicate that they are good quenchers for the Mn^{2+} luminescence of the hybrid. The near zero value of *b* in the fitting also implied that the quench was confirmed to the theortical S-V equation. The fitted K_{SV} of CV was greatest, RB5 next and BX least, which is just the reverse to the linear response range of Log *I*-*c* plots. It is understandable that the smaller Ksv of a quencher give a broader linear response range for detection.

3.5 The sensoring repeatability of the hybrid thin film

As a fluorescence sensor, the reversibility was crucial for its application. Differing from the fluorescence probing method base on intermolecular interaction such as electron transfer or energy transfer, the IFE is a typical photophysical effect, free of the interaction between the fluorphore and the absorbents, and is favorable for its reversible sensoring implementation and device design. As shown in Figure 5 , this hybrid thin film show good sensoring reversibly for CV, the luminescence quench/recover cycle can be implemented upto 10 times without any obvious luminescence degrade. The quenched fluorescence will recover after rinsed by deionized water. The hybrid thin film also exhibit the

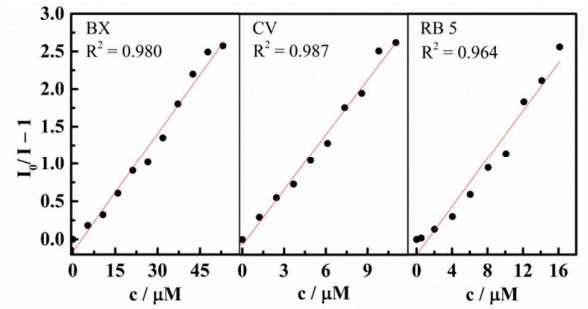

Figure 4. The Stern-Volmer plot of the Mn^{2+} luminescence in hybrid thin film by three species solution at pH = 7 , I_0 and I are the initial and observed luminescence intensity, respectively.

Table 2 The Stern-Volmer plot parameters in Figure 4

	K_{SV}/(L/mol)*	*b**	Linear range /μM	R^2
BX	5.232×10^4	-1.650×10^{-1}	0 – 53.10	0.980
CV	2.441×10^5	-7.341×10^{-2}	0 – 11.03	0.987
RB5	1.592×10^5	-2.002×10^{-1}	0 – 16.13	0.964

* The fitting equation was :$I_0/I - 1 = K_{SV}c + b$, R^2 :correlation coefficient

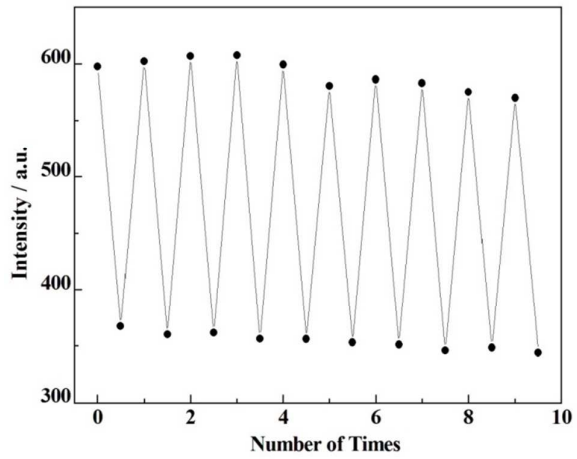

Figure 5. The cycle reversibility of the Mn2+ luminescence in the hybrid thin film for probing the CV aqueous solution(4.43μM)

reversible response to BX and RB5 solution (Fig.S1, S2, in ESI). In fact, other hybrid was also tried to fabricate thin film for IFE investigation, such as $(Zn_{0.95}Mn_{0.05}Se)_2$·*oa*, however, its unstable Mn^{2+} luminescence make it failed for the reversible measurement and can not be used as an IFE-based sensor. As far as the thermal stability of the luminescence, it can be found that the Mn^{2+} luminescence was stable below 80 °C, and can be used in luminescence sensoring for environmental pollutants(Fig.S3, in ESI).

Furthermore, this hybrid thin film was surface hydrophobic due to the long octyl group of *oa* molecules, and when dipped into the aqueous solution, the solution can not wet the film surface throughout. This surface hydrophobicity was favorable for the rapid luminescence recovery for next detection based on IFE, which was impossible for other fluorescence method based on intermolecular interaction mechanism(e.g. FRET). As far as the pH stablity is concerned, this Mn^{2+} luminescence of the hybrid was unstable when the solution was acidic enough or alkline enough. It was found that the 597 nm luminescence remain intact and pH-independent during the pH value from 4 to 10 (Fig. S4). In acidic solution(e.g. pH = 2), the hybrid will decompose to release ammonia, and in strong alkaline solution (e.g. pH = 12), the intensity of the 597 nm luminsecence will fell and other unknown peak will appear. Although this limit, it can be concluded that this hybrid thin film can probe in various aqueous solution environments with pH value ranging from 4 to 10.

4 Conclusions

In summary, the pure and well-crystalline $(Zn_{0.95}Mn_{0.05}S)_2$·oa (oa = octylamine) I/O hybrid was prepared by solvothermal synthesis at 170 °C for 5-7 days, the grey hybrid sheets with micrometer size was obtained, and its thin films was fabricated by drop-casting method. The thin film was orientated with the normal of all the hybrid sheets and smooth and continuous, confirmed by SEM observation. Its fluorescence properties was characterized, which indicated a strong absorption at 300 nm and the Mn^{2+} fluorescence at 597 nm, and the optimal fluorescence was obtained for the 5 at% Mn^{2+} doping content. The luminescence inner filter effect (IFE) of the thin film was verified and investigated. The hybrid thin film was sensitive enough to monitor the concentration of three selected environmental contaminant The Log*I* - *c* and Stern-Volmer plots showed the linear relationship at μM scale with the broadest range for BX detection(0 – 53.10 μM) and the smallest Ksv (52320 L/mol). Moreover, this hybrid thin film was surface hydrophobic and was favorable for the rapid luminescence recovery in multiple IFE-based detections. The Mn^{2+} luminecence at 597 nm for detection show good cycle reversiblity upto 10 times and this luminescence was stable when detecting the aqueous solution with pH ranging from 4 to 10, which is the case for the ordinary water environmental sample.

This work indicated that this $(Zn_{0.95}Mn_{0.05}S)_2$·*oa* hybrid thin film can serve as a novel and feasible IFE fluorescence sensor for probing occurrence of these selected environmental contaminant species at the μM scale, and it is also suitable for probing other species meeting the requirment of the IFE. The hybrid thin film is low cost, easy to prepare, and good photo/chemical stability. Their fluorescent probe based on the IFE provides obvious advantages of simplicity, convenience, and rapid implementation and thus has potential application for the detection in the environmental analysis. However, there are still some problems needs further study including the luminescence quench mechanism, the IFE for other hybrid and for the excitation and emission, and so on.

Acknowledgements

This work was supported by the Fundamental Research Funds for the Central Universities of China.

Notes and references

1 M. O. Palmier and S. R. Van Doren, *Anal. Biochem.*, 2007, **371**, 43.

2 T. Larsson, M. Wedborg and D. Turner, *Anal. Chim. Acta*, 2007, **583**, 357.
3 P. L. Cary, P. D. Whitter, C. A. Johnson, *Clin. Chem.* 1 984, **30**, 1867.
4 X. Yan, H. Li, Y. Li and X. Su, *Anal. Chim. Acta*, 2014, **852**, 189.
5 M. Zheng, Z. Xie, D. Qu, D. Li, P. Du, X. Jing and Z. Sun, *ACS Appl. Mater. Inter.*, 2013, **5**, 13242.
6 A. Vujacic, V. Vasic, M. Dramicanin, S. P. Sovilj, N. Bibic, S. Milonjic and V. Vodnik, *J. Phys. Chem. C*, 2013, **117**, 6567.
7 L. Shang and S. Dong, *Anal. Chem.*, 2009, **81**, 1465.
8 S. Yang, C. Wang, C. Liu, Y. Wang, Y. Xiao, J. Li, and R. Yang, *Anal. Chem.* 2014, **86**, 7931.
9 C. Moon, G. M. Dalpian, Y. Zhang and S. Wei, *Chem. Mater.*, 2006, **18**, 2805.
10 H. X. Fu and J. Li, *J. Chem. Phys.*, 2004, **120**, 6721.
11 C. N. R. Rao, A. K. Cheetham and A. Thirumurugan, *J. Phys-Condens. Mater.*, 2008, **20**, 1.
12 K. D. Karlin, *Progress In Inorganic Chemistry*, ed. J. Li and R. Zhang, John Wiley & Sons Inc, Hoboken, 2012, **57**, 445.
13 X. Zhang, M. Hejazi, S. J. Thiagarajan, W. R. Woerner, D. Banerjee, T. J. Emge, W. Xu, S. J. Teat, Q. Gong, A. Safari, R. Yang, J. B. Parise and J. Li, *J. Am. Chem. Soc.*,2013, **135**, 17401.
14 X. Huang and J. Li, *J. Am. Chem. Soc.*, 2007, **129**, 3157.
15 X. Y. Huang, J. Li, Y. Zhang and A. Mascarenhas, *J. Am. Chem. Soc.*, 2003, **125**, 7049.
16 H. Yao, X. Li, S. Ai and S. Yu, *Nano. Res.*, 2010, **3**, 81.
17 H. Yao, M. Gao and S. Yu, *Nanoscale*, 2010, **2**, 323.
18 J. Lu, S. Wei, Y. Y. Peng, W. C. Yu and Y. T. Qian, *J. Phys. Chem. B*, 2003, **107**, 3427.
19 X. Zhang, Y. Ren, M. Roushan and J. Li, *Eur. J. Inorg. Chem.*, 2012, **135**, 5966.
20 X. Huang, M. Roushan, T. J. Emge, W. Bi, S. Thiagarajan, J. Cheng, R. Yang and J. Li, *Angew. Chem. Int. Ed.*, 2009, **48**, 7871.
21 J. Li, W. Bi, W. Ki, X. Huang and S. Reddy, *J. Am. Chem. Soc.*, 2007, **129**, 14140.
22 H. Yao, X. Zhang, X. Wang, S. Yu and J. Li, *Dalton Trans.*, 2011, **40**, 3191.
23 W. T. Yao, S. H. Yu, L. Pan, J. Li, Q. S. Wu, L. Zhang and H. Jiang, *Small*, 2005, **1**, 320.
24 S. Wei, J. Lu and Y. Qian, *Chem. Mater.*, 2008, **20**, 7220.
25 J. Lu, S. Wei, W. C. Yu, H. B. Zhang and Y. T. Qian, *Chem. Mater.*, 2005, **17**, 1698.
26 X. Fang, M. Roushan, R. Zhang, J. Peng, H. Zeng and J. Li, *Chem. Mater.*, 2012, **24**, 1710.
27 M. Roushan, X. Zhang and J. Li, *Angew. Chem. Int. Edit.*, 2012, **51**, 436.
28 W. Ki, J. Li, G. Eda and M. Chhowalla, *J. Mater. Chem.*, 2010, **20**, 10676.
29 S. Wei, J. Peng, M. Wang, X. Fang, Y. Fan, X. Li and J. Lu, *Chem. Commun.*, 2012, **48**, 4615.
30 Q. Gao, S. Wang, H. Fang, J. Weng, Y. Zhang, J. Mao and Y. Tang, *J. Mater. Chem.*, 2012, **22**, 4709.
31 J. Kim, M. R. Kim, S. Park and D. Jang, *Cryst. Eng. Comm.*, 2010, **12**, 1803.
32 Y. K. Chang, J. E. Chang and L. C. Chiang, *Chemosphere*, 2003, 52, 1089.
33 A. Vujacic, V. Vasic, M. Dramicanin, S. P. Sovilj, N. Bibic, S. Milonjic and V. Vodnik, *J. Phys.Chem. C*, 2013, **117**, 6567.
34 K. Sahel, N. Perol, H. Chermette, C. Bordes, Z. Derriche and C. Guillard, *Appl Catal B-Environ.*, 2007, **77**, 100.